Dynamics Testing and Simulation of Inflatable Deployable Membrane Antennas

Wei Jianzheng[1]*, Yu Lin[1], Jiang Yu[2], Tan Huifeng[1], zhang Jinxiu[2]

(1 Center for Composite Materials, Harbin Institute of Technology, Harbin, R.P. China, 150080,

*weijz@hit.edu.cn)

(2 School of Astronautics, Harbin Institute of Technology, Harbin, R.P. China, 150080)

Abstract：The inflatable deployable membrane antenna structures have many advantages such as small folding size, high reliability and low cost. The structure mainly consists of its center hub, thin-plate ribs, inflatable thermo-curing torus, reflected membrane and inflation control system. This paper establishes a deployable system to simulate zero-gravity based on the parabolic membrane antenna with inflatable torus and tests the deployable process. The shell-membranes finite element model of the antenna structures is modeled to simulate of the dynamics characters of the structure. After that the effects of the different inflatable pressure inside its support torus, the temperature of thermos-curing on the dynamic characteristics are also discussed. Finally, the dynamic characters of the inflatable antenna was tested on the condition of the horizontal suspension system with 12 elastic strings and the fully structural vibrational frequency were given, and the mode of vibration and damping ratio was verified to the correctness of the simulation method. These results provide the reference for the design of inflatable deployment antenna structures.

Keyword：Dynamics Testing, Membrane antenna, Inflatable, Deployment

1Introduction

It is a development tendency to develop reflector with large apertures and high accuracy [1,2] which have the potential to offer an ideal solution for large apertures reflector[3]. Reflectors with large aperture radiate more energy than smaller ones and reflectors accuracy determines whether an antenna iscapable of the scheduled requirements. Although inflatable antennas have been considered since In the 1960s, inflatable antennas was successful deployed for L and S band applications[4], now interest is turning to such antennas shorter wavelength bands. After data transmission rates of communication in near-Earth-orbit and deep-space missions reach hundreds of megabits per second, the diameter of the aperture may need to reach 10 m or more to support that rates [5].However, larger reflectors typically means heavier weight, the less folded efficiency, so it is difficult to design a large reflector that can be folded and deployed several times after which the surface accuracy is still competent. Puig et al. conduct a preliminary FE(Finite Element) analysis using Nastran/Patron ona typical deployable truss structure in an astrophysics mission requiring a focal length extension.[3]Hu et al. develop a Fully-Cartesian-coordinate (FCC) method using Cartesian coordinates of points and Cartesian components of unitary vector to describe three-dimension mechanism large deployable structures. Guan et al. [6]analyze the static deformation of the synchronism deployable antenna consists of tetrahedral elements from central element.[7]Wang et al. analyzed the wrinkling of membrane with a new modified displacement

component method and made an influence parameter analysis and wrinkling control for inflatable reflectors. In this paper[8], an inflatable deployable paraboloid reflector(IDPR)was fabricated[9] which compromise the advantages of three kinds reflector: the truss reflector[10], the rib reflector [11, 12], and the inflatable reflector[13]. As far as structure dynamics concerned, in 2011, Pazhooh employed a non-contacting electromagnetic exciter and two laser displacement sensors[14]. The identified frequencies of the present study were higher than the measured frequencies by Ruggiero et al.[15], which indicated that the modal experiment of the SRT proved that dynamic testing of this structure was very challenging. In 2013, tan used hammer and tri-axial accelerometers for experimental modal test on inflatable membrane torus, and extracted the former 8 in-plane modes and the former 6 out-of-plane modes[16]. Compared to noncontact method in Pazhooh, Song and Ruggiero, impact hammer provided more energy for higher modes. As the inflatable deployable reflector antenna is much larger than inflatable torus, more energy is needed for global vibration.

In conclusion, modal test on space membrane structure is still very challenging. A scale model in vacuum condition with a scanning laser Doppler vibrometer is good way to minimize the effect of air during testing, but it will be problematic for a large-scale full size antenna as the total cost increase sharply.

2 Structure of the inflatable deployable membrane antenna

The main part of the inflatable deplorable membrane antenna is the deployable reflector, which is the key component that makes the antenna suitable for the scheduled requirements. Also, the antenna contains other component such as inflate system, packing system and sub-reflector supporting system. The deployable reflector is supported by the supporting system consisting of a central hub, the supporting ribs, an inflatable torus and the tension system. (Fig 1)

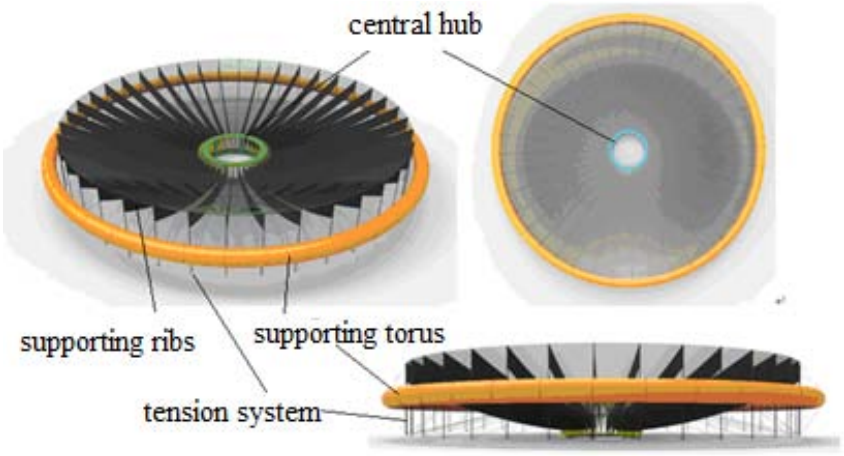

Figure 1 Design diagram of the inflatable deployable membrane antenna

The reflector is the main functional part which can send and receive the electrical signal. To achieve a better working condition, the material of the reflector should be flexible and have the property of resilience after folding. Here, the desired material is the mesh knitted by the gold-coated molybdenum wires, which may almost achieve all functions of the reflector.

The central hub (Fig. 2) is located in the center of the reflector, around which the support ribs are extended. The outermost component of reflector is the support torus (Fig. 3), which is connected with support ribs by the tension system. The reflecting surface is biaxial tensioned and hung on the ribs (Fig. 4).With the aid of the central hub, the ribs can be located and oriented in the supporting system. As the foundation of the inflatable reflector, the precision of the central hub have effect on

the other components and the final RMS of the reflector. The number of the supporting rib is chosen as 24 and the angle between the neighbor ribs is 15 degree. Here, the desired material of the rib is the carbon-fiber laminate. The shape of the rib, which directly influences surface accuracy, is maintained and controlled by the tension of the torus. The morphing of the rib has different performances in different tensions. To avoid the out plane buckling of the rib, the tension system is introduced. The location of the tension system is chosen base on the method proposed by Wang [9]. The tension system transfer tension between the ribs and torus and control the shape of the rib. In the working status, the shape of rib, which is in the pretension state, should be the assigned shape.

Based on the structure aforementioned, an inflatable deployable paraboloid reflector with aperture of 3m and aΦ3.2m torus was fabricated to validate the foldability and the ability to deploy experimentally.

Figure 2 The central hub's design diagram

1) folded 2) deployed

Figure 3 The supporting torus in folded and deployed configurations

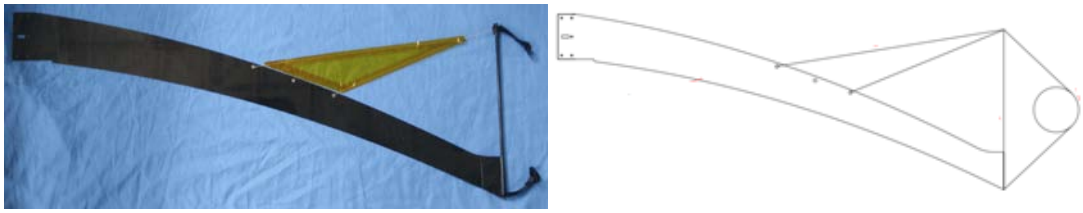

Figure 4 The supporting rib and its design diagram

3 Testing of folding and deployment of the membrane antenna

In order to save the cost of launching, the size of the antenna after packing should be minimized. The presented inflatable reflector achieve the foldability form the flexibility of its component, while the deploy process is driven by the inner pressure in the torus.

The experiments of fold and deploy of the inflatable deployable paraboloid reflector conducted on the ground utilizing the gravity-free simulating system (Fig. 5) confirm that the inflatable reflector can endure tens of times of folding and deploying. The main part of the gravity-free simulating

system is a rigid frame fixed to the ground, and a brunch of elastic ropes was dropped from the sliding groove on the frame. While the lower end of the elastic rope were attached to the ribs and the torus. The stiffness of the elastic rope was chosen in advance to reduce the deflection of the ribs while folding.

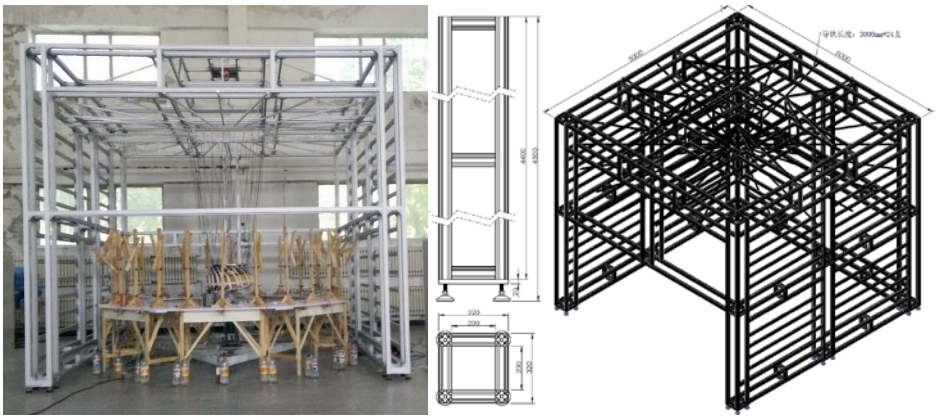

Figure 5 The gravity-free simulating system and its design diagram

3.1 Folding

To minimize the volume the inflatable reflector, ribs are wrapped around the central hub during folding process. In this process, the evenly distribution and the neatness of the ribs are the difficult points. A pump is used to pump the air out of the torus from two air taps on the opposite position of the supporting torus. And the torus was folded in a zigzag pattern. Due to the limitation of the gas speed of the inflating, the process of folding start at the center of two air taps. The asynchrony of the ribs and torus folding will cause the uneven intervals between two ribs. So the monitor of the ribs' shapes in the folding process is necessary and adjustments of the ribs' shape should be made while pumping. (Fig. 6) In the folding process the ribs were bended to the outer boundary of the central hub in which a certain amount of strain energy was gathered and stored in the ribs. So a woven ribbon was used to packing the folded inflatable reflector. (Fig. 7)

Figure 6 Adjusting the shape and the distribution of the ribs

1) top view 2) bottom view

Figure 7 Inflatable membrane antenna after folding

3.2 Inflatable deployment

According to the main driven force in the deployment, the process of deploying can be divided to two sub-process. The first sub-process is mainly driven by the strain energy stored in the ribs and torus, while in the second sub-process the inflatable reflector obtain the power from the inflating gas.

The first step to deploy the folded inflatable reflector was the release the woven ribbon. Upon release of the ribbon, the stored strain energy caused the wrapped ribs to spring to their stiff, deployed shape. But the volume of the initial inflating gas prevented the fully deployment of the torus, so the ribs were constrained by the half-deployed torus and a small portion of the stain energy was still left in the deformed ribs. This sub-process only took about 1s to release the large portion of the strain energy, so an impact load was exerted to the inflatable reflector. The impact load should be taken into consideration in the design procedure. Figure 8 shows the inflatable reflector at the start and the end of the sub-process.

1) At the start of the sub-process 2) At the end of the sub-process

Figure 8Strain energy driven deploying sub-process

In the second sub-process, the torus was inflated and the tension of the torus drives these ribs to deploy further to reach the assigned shape. In this sub-process the remained strain energy was released thoroughly. And the driven force of the inflating changed to the inner gas pressure. The inner pressure was determined by the total gas volume in the torus. So we could manipulated the total deploying time by adjusting the speed of the inflating gas. In the fabrication of the torus, the

inner diameter of the air tap was chosen as 5mm to reduce the weight as the air tap is mainly made of copper. The speed of the inflating gas is limited by the cross section area of the air tap, so the total deploying time is mainly depended on the inflating speed.

At the beginning of the sub-process, the zigzag pattern near the air tap started to inflate because of the local higher pressure. As the inner pressure become higher and higher, the torus expanded to a round circle, and the inner volume of the torus formed a wholly connected space. In the meantime, the ribs followed the torus to realize the deployment.

At the end of the sub-process, the inflatable reflector was fully deployed and the final inner pressure reached 20kPa. The tension system transfer the force from the torus to the ribs, resulting an expected configuration and precision. The sub-process driven by the inner gas pressure is depicted in the Fig. 9.

Figure 9 Inner gas pressure driven deploying sub-process

The experiments of folding and deploying of the inflatable deployable paraboloid reflector were conducted 5 times, and the average time consuming isrecorded and calculated. The main event in the sequence of the deployment is listed in the Table 1, so as the corresponding time nodes. The average time of fully deployment of the inflatable reflector is about 10 min. And the successive deployment of the inflatable reflector give evidence of the high-speed, the reliability and durability of the inflatable reflector fabricated.

Table 1Sequence of the deployment and time nodes

No.	Time*	Event

	（Initial as 0, min）	
1	0	Ribbon released, deployment begins
2	2	Zigzag pattern straightened
3	5	Inner volume of torus wholly connected
4	7	Torus fully deployed, inner pressure rises
4	10	Inner pressure reach 20kPa，deployment ends

* Average time of 5 deployments

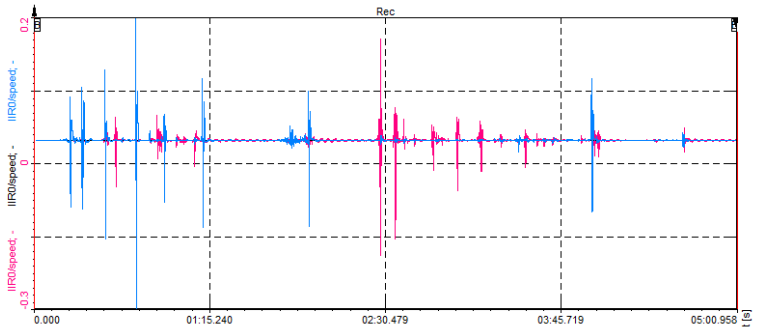

Figure 10Curve of deployment velocity for the IDPR

The acceleration of one point on the torus was measured and the deploying speed of the torus was gathered by integrating and averaging the acceleration. The results show that the maximum speed in circumferential direction and normal direction is 0.2m/s and -0.3m/s, respectively. (Fig.10)

4 Dynamics testing

4.1 Testing methods

During the dynamic test, the IPDR is fully deployed and hung on the gravity-free simulating system. The hanging point is evenly distributed on the inflatable torus. The acceleration transducers are mounted on the middle and the outer border of the alternative ribs and corresponding point on the torus in the corresponding direction as shown in the Fig. 11. In the dynamics test, to avoid the frequency of the rigid body, two additional acceleration transducers are mounted the central hub. For each acceleration transducer, the acceleration in *x, y*, *z* directions are captured and the overall response in 114 channels describe the dynamics characteristic of the IDPR. The knocking points and the directions of the force hammer locate on the outer edge of the No. 1 rib in the vertical direction and on the outer edge of the central hub in the vertical, normal, tangential directions. The geometry, active point, transducer location, and the directions of the response point are depicted in the Fig. 11.

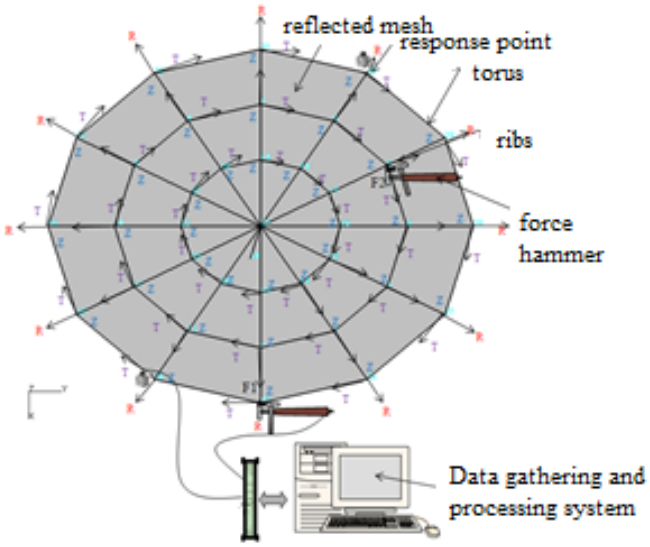

Figure 11Model testing methods for the IDPA

4.2 Testing results

The dynamic response of the IDPR is tested under two circumstances. Figure 12 and Table 2 depict the response of the IDPR when the inflatable torus was heated up to and kept at the glass transition temperature (T_g), 70°C and the inner pressure was kept at10.0kPa (circumstances I). When the temperature of the torus came to 25°C and got cured, and the pressure in the torus was 0Pa meaning that the torus and the IDPR was totally self-supported (circumstances II), the response of the IDPR was shown in Fig. 13 and Table 3.

The first order frequency and damp ratio of the IDPR are6.81Hz and 6.07%respectively when the torus is kept at the T_g and inner pressure. The first order frequency and damp ratio of the IDPR are 6.41Hzand 6.93% respectively after the torus got cured. The difference is so small that the torus satisfy the design requirements.

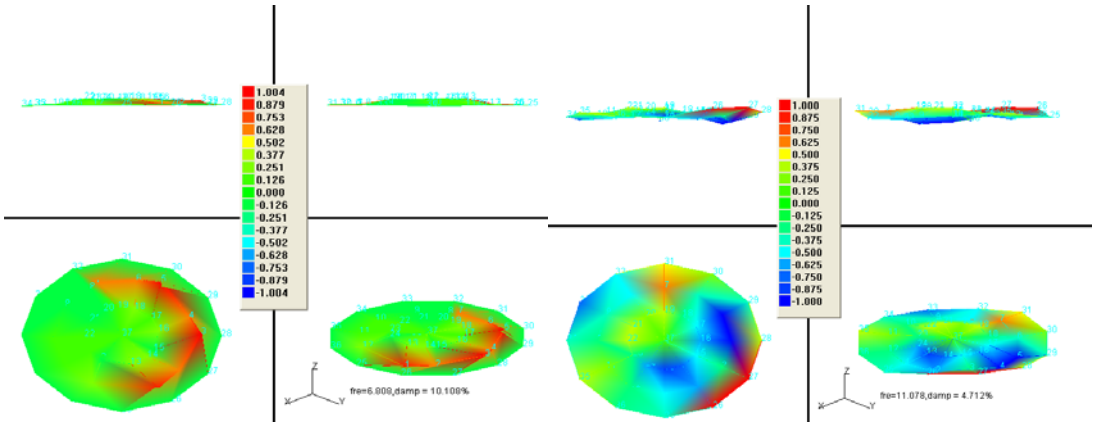

Figure 12Mode of vibration: 1st order torsion and 1st order bend (circumstances I)

Table 2 Test result undercircumstances I

Order	Frequency (Hz)	Damp ratio (%)	Mode of vibration
1	6.81	6.07	1st order torsion (average over the ribs, local modes between4Hz and 8Hz exist）

2	11.08	4.71	1st order bend
3	24.84	3.64	2nd order torsion
4	29.20	2.86	3rd order torsion

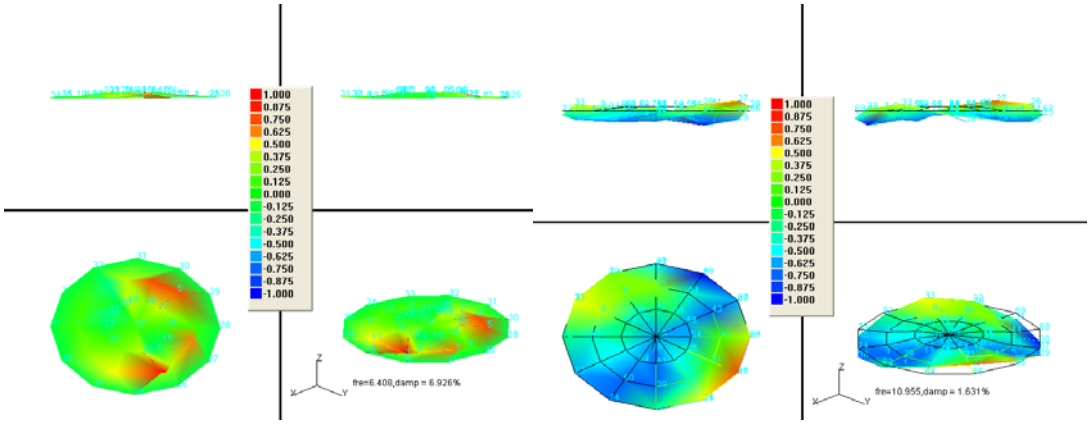

Figure 1314Mode of vibration: 1st order torsion and 1st order bend (circumstances II)

Table 3 Test result under circumstances II

Order	Frequency (Hz)	Damp ratio (%)	mode of vibration
1	6.41	6.93	1st order torsion (average over the ribs, local modes between3.75Hz and 8Hz exist）
2	10.96	1.63	1st order bend

5 Conclusions

An inflatable deployable membrane antenna was fabricated and the design method was testified. The experiments of folding and deploying of the inflatable reflector were conducted with the assistance of the gravity-free simulating system for multiple times. A series of successive experiments test and verify the reliability and durability of the inflatable membrane antenna. The average time to fully deploy the inflatable reflector is about 10min, which enable the fast deployment in the orbit. In the lower order, the mode of the IDPR is mainly displayed as torsion mode. And the difference in dynamic response between the circumstances (high temperature at T_g and with inner pressure vs. cured torus with 0 pressure) is not obvious, showing that the IDPR with the cured torus meet the design requirements.

6 Reference

1. Meguro, A., Harada, S., and Watanabe, M., “Key Technologies for High-Accuracy Large Mesh Antenna Reflectors,” Acta Astronautica, Vol. 53, No. 11, 2003, pp. 899–908. doi:10.1016/S0094-5765(02)00211-4
2. Lane, S. A., Murphey, T. W., and Zatman, M., “Overview of the Innovative Space-Based Radar Antenna Technology Program,” Journal of Spacecraft and Rockets, Vol. 48, No. 1, 2011, pp. 135–145.
3. L. Puig, A. Barton, N. Rando, A review on large deployable structures for astrophysics missions, Acta Astronautica, Volume 67, Issues 1–2, July–August 2010, Pages 12-26, ISSN 0094-5765.
4. Thomson, M. W., “Astromesh Deployable Reflectors for Ku and Ka Band Commercial Satellites,”

AIAA Paper 2002-2032, 2002.

5. Michael J. Coleman, Frank Baginski, and Robert R. Roman of sky. "Effect of Boundary Support and Reflector Dimensions on Inflatable Parabolic Antenna Performance", Journal of Spacecraft and Rockets, Vol. 49, No. 5 (2012), pp. 905-914.
6. Hu Qi-biao, Guan Fu-ling, Hou Peng-fei. J. Zhejiang Univ. Sci. A (2001) 2: 152. doi:10.1631/jzus.2001.0152
7. Guan F., Shou J., Hou G. et al. J. Zhejiang Univ. - Sci. A (2006) 7: 1365. doi:10.1631/jzus.2006.A1365
8. Wang C.G., Mao L.N., Du X.W., and He X. D., "Influence Parameter Analysis and Wrinkling Control of Space Membrane Structures," Mechanics of Advanced Materials and Structures, Vol. 17, No. 1, 2010, pp. 49–59.
9. Wang C. G., Xia Z. M., and Tan H. F. "Initial Shape Design and Stability Analysis of Rib for Inflatable Deployable Reflector", AIAA Journal, Vol. 53, No. 2 (2015), pp. 486-492.Xia
10. Xu, Y., Guan, F. L., Chen, J. J., and Zheng, Y., "Structural Design and Static Analysis of a Double-Ring Deployable Truss for Mesh Antennas," Acta Astronautica, Vol. 81, No. 2, 2011, pp. 545 – 554.
11. Tan, L. T., and Pellegrino, S., "Thin-Shell Deployable Reflectors with Collapsible Stiffeners: Experiments and Simulations," AIAA Journal, Vol. 50, No. 3, 2012, pp. 6
12. James Pearson, James Moore, and Houfei Fang. "Large and High Precision Inflatable Membrane Reflector", 51st AIAA/ASME/ASCE/AHS/ASC Structures, Structural Dynamics, and Materials Conference, Structures, Structural Dynamics, and Materials and Co-located Conferences, 2010.
13. Soykasap, O, and Tan, L. T., "High-Precision Offset Stiffened Springback Composite Reflectors," AIAA Journal, Vol. 49, No. 10, 2011, pp. 2144 – 2151.
14. M. D. Pazhooh, M.A. Dokainish, S. Ziada. Experimental modal analysis of an inflatable, self-rigidizing toroidal satellite component[C]. In T. Proulx (ed.), Experimental and Applied Mechanics, Volume 6, Conference Proceedings of the Society for Experimental Mechanics Series 9999, DOI 10.1007/978-1-4614-0222-0_23.
15. E. J. Ruggiero, D.J. Inman. Gossamer spacecraft: recent trends in design, analysis, experimentation, and control [J]. Journal of spacecraft and rockets. 2006，43(1)：10-24.
16. H. F. Tan, Y. L. Li, C. Q. Miao. Progress in dynamic analysis of space inflatable structure [J], Chinese Journal of Advance in Mechanics. 2007，37(2)：214-224